

# Analytical expressions for water-to-air stopping-power ratios relevant for accurate dosimetry in particle therapy

Armin Lühr<sup>1,2</sup>, David C. Hansen<sup>2</sup>, Oliver Jäkel<sup>3,4</sup>, Nikolai Sobolevsky<sup>5</sup>, and Niels Bassler<sup>1,2</sup>

<sup>1</sup> Department of Experimental Clinical Oncology, Aarhus University Hospital, Aarhus, Denmark

<sup>2</sup> Department of Physics and Astronomy, University of Aarhus, Aarhus, Denmark

<sup>3</sup> Department of Medical Physics in Radiation Oncology, German Cancer Research Center (DKFZ), Heidelberg, Germany

<sup>4</sup> Heidelberg Ion Beam Therapy Center (HIT), Heidelberg University Hospital, Heidelberg, Germany

<sup>5</sup> Department of Neutron Research, Institute for Nuclear Research of the Russian Academy of Sciences, Moscow 117312, Russia

E-mail: luehr@phys.au.dk; bassler@phys.au.dk

## Abstract

**Abstract.** In particle therapy, knowledge of the stopping-power ratio (STPR) of the ion beam for water and air is necessary for accurate ionization chamber dosimetry. Earlier work has investigated the STPR for pristine carbon ion beams, but here we expand the calculations to a range of ions ( $1 \leq z \leq 18$ ) as well as spread out Bragg peaks (SOBPs) and provide a theoretical in-depth study with a special focus on the parameter regime relevant for particle therapy.

The Monte Carlo transport code SHIELD-HIT is used to calculate complete particle-fluence spectra which are required for determining STPR according to the recommendations of the International Atomic Energy Agency (IAEA).

The STPR at a depth  $d$  depends primarily on the average energy of the primary ions at  $d$  rather than on their charge  $z$  or absolute position in the medium. However, STPRs for different sets of stopping-power data for water and air recommended by the International Commission on Radiation Units & Measurements (ICRU) are compared, including also the recently revised data for water, yielding deviations up to 2% in the plateau region. In comparison, the influence of the secondary particle spectra on the STPR is about two orders of magnitude smaller in the whole region up till the practical range. The gained insights enable us to propose simple analytical expressions for the STPR for both pristine and SOBPs as a function of penetration depth depending parametrically on the practical range.

PACS numbers: 87.55.Qr, 34.50.Bw, 87.53.Bn, 87.55.K-

## 1. Introduction

Stopping powers are essential for calculating the dose deposited by ionizing particles. The deposited dose is described as the mass stopping power multiplied with the particle fluence, while assuming charged particle equilibrium from the short-ranged delta electrons. At particle-therapy centers air-filled ionization chambers are routinely used as a main tool for quality assurance of the delivered beam. Several dosimetry protocols for protons have been conceived while the most recent protocol provided by the International Atomic Energy Agency (IAEA), TRS-398 [1], sets the standard in proton dosimetry today. In addition, TRS-398 also covers dosimetry for ions heavier than protons. The protocol uses an absorbed dose-to-water based formalism and relates the dose to water  $D_{w,Q}$  to the acquired charge  $M_Q$  multiplied by a calibration factor  $N_{D,w,Q_0}$  and a dimensionless beam quality correction factor  $k_{Q,Q_0}$ . The correction factor  $k_{Q,Q_0}$  relates the measured beam quality  $Q$  to the beam quality  $Q_0$  used for calibration of the dosimeter and it is defined in TRS-398 as

$$k_{Q,Q_0} = \frac{(S_{\text{water/air}})_Q (W_{\text{air}})_Q p_Q}{(S_{\text{water/air}})_{Q_0} (W_{\text{air}})_{Q_0} p_{Q_0}} \quad (1)$$

including the water-to-air stopping-power ratio,  $S_{\text{water/air}}$ , the mean energy expended in air per ion pair formed,  $W_{\text{air}}$ , and a perturbation factor  $p_Q/p_{Q_0}$  which considers effects for the specific ionization chamber used.

As mentioned in TRS-398, calculating the correct beam quality factor in particle therapy is complex since it involves knowledge of the entire particle-energy spectrum at the point of interest. Instead, TRS-398 proposes a pragmatic approach by recommending a fixed value of 1.13 as a generic correction factor for the dosimetry of ions heavier than protons based on the analysis by Hartmann *et al.* [2], irrespective of the particle types and energy spectra which are functions of depth. Accordingly, TRS-398 summarizes that the estimated combined standard uncertainty in  $k_{Q,Q_0}$  in ion beams heavier than protons (about 3%) arises largely from the uncertainty of the stopping-power ratio (STPR) (about 2%) and the value for  $W_{\text{air}}$  (about 1.5%).<sup>‡</sup> This has been taken up by Henkner *et al.* [3] and Geithner *et al.* [4, 5] for mono energetic *carbon* beams, and they found out that (i) the STPR is not constant but varies with penetration depth, and (ii) it depends strongly on the accuracy of the stopping-power data used as input for the calculation. Accordingly, it was concluded that in a clinical setting an over or under dosage may occur in the order of a few percent.

Here, we shall continue the initiated work on STPRs focusing on two objectives. First, gaining a sound understanding of the physics determining the STPR, and second, exploiting the gained understanding in order to provide results with direct clinical relevance which are ready to be applied in clinical practice in a quality assurance setting.

The deeper insight in the context of STPR is required since STPR strongly depends on the stopping-power data which are used for its determination. The problem is,

<sup>‡</sup> Although the study of the value for  $W_{\text{air}}$  is beyond the scope of this work it shall be mentioned that the estimated uncertainty for  $W_{\text{air}}$  calls for a detailed investigation.

however, that the stopping-power data currently recommended by the International Commission on Radiation Units and Measurements (ICRU) possess some intrinsic inconsistencies. In contrast to an accurate but purely numerical calculation of STPRs, a sound understanding of the relevant physics allows for conclusions independent of the employed set of stopping-power data. It is also a prerequisite for an analytical description of the STPR. It should be emphasized that, in contrast to earlier work on STPR [3–5], the present study also considers the recently revised ICRU 73 [6] stopping-power data for ions heavier than helium on water. These data replace the ones originally published in ICRU 73 which led to a still ongoing discussion on stopping powers for water targets (see, e.g., [7]) especially in view of recent measurements by Schardt *et al.* [8].

TRS-398 explicitly states that the STPR for water-to-air,  $S_{\text{water/air}}$ , should be obtained by averaging over the complete spectra of particles present. And consequently, this requirement was considered to be an important limitation in the case of heavy charged particles, where the determination of all possible particle spectra was assumed to be a considerable undertaking. This was certainly the case a decade ago and may still be true from the point of view of dose determination for routinely quality assurance. Nowadays, however, the determination of complete spectra of particles can be achieved conveniently and with high accuracy by applying Monte Carlo transportation codes exploiting the commonly available computer power. These codes are in general valuable in predicting radiation fields of ions in tissues and are in particular useful in hadron therapy for the simulation of ion transport. The most common codes in particle therapy with ions heavier than protons are Geant4 [9], FLUKA [10], PHITS [11], MCNPX [12], and SHIELD-HIT [13, 14], all taking into account the atomic interaction of the ions with the target medium as well as the nuclear interaction. It is the former interaction which mainly determines the energy loss of the incident ions and therefore the stopping power, while the latter interaction is responsible for fragmentation and therefore for the production of secondary-particle spectra.

Initial studies on STPRs relevant for dosimetry in radiation therapy with ions heavier than protons were performed without Monte Carlo calculations ignoring the influence of the secondary particle spectrum (e.g. [15–17] as presented in TRS-398 [1]). Calculations exploiting the capabilities of Monte Carlo codes were performed with SHIELD-HIT but exclusively carbon-ion fields [3–5] were studied. However, the dependence of the STPR on different ion species is of interest since a number of facilities world-wide (e.g., NIRS and HIT) are equipped with radiation fields which cover a broader range of ions than merely protons and carbon ions. Furthermore, it was recently argued that ions heavier than carbon may play an important role in the near future concerning the radiation therapy of radio-resistant tumors [18]. Consequently, a large variety of ion species, namely, H, He, Li, C, N, O, Ne, Si, and Ar are considered here — all accessible either for clinical radiation therapy (up till O and Ne at HIT and NIRS, respectively) or for in vitro radiobiology experiments.

Despite their obvious relevance in medical application, so far, STPRs for spread-out Bragg peaks (SOBPs) for ions heavier than protons have been discussed only scarcely

in literature, namely, by Henkner *et al.* [3]. In the case of proton beams more detailed efforts have been performed, e.g., by Palmans *et al.* [19,20] and earlier already by Medin and Andreo [21]. Henkner *et al.*, who considered carbon ions, outlined in the conclusions of [3] that a more detailed analysis of STPRs for SOBPs is clearly needed since their statements were only based on the analysis of a single *physically* optimized SOBP using one set of stopping-power data. Consequently, one focus of this work should be a systematic study of the STPR for SOBPs, both *physically* and *biologically* optimized, of different widths and practical ranges leading to an analytic expression for the STPR.

This paper is organized as follows: First, the physics relevant for the STPR and the employed methods are discussed. Furthermore, analytical expressions for the average energy of the primary ions and STPRs are proposed. Subsequently, the results for the water-to-air STPR for pristine as well as SOBPs are presented and compared to the proposed analytical expressions. The following discussion concentrates on three issues, namely, the influence of the stopping-power data on the STPR, the dependence of the STPR on the ion energy, and STPRs for SOBP.

## 2. Materials and Methods

For all our calculations we used the Monte Carlo particle transport code SHIELD-HIT [5, 14], based upon the most recent version SHIELD-HIT08 [22]. A number of improvements and new functionalities were added to SHIELD-HIT08, documented in [23], finally resulting in SHIELD-HIT10A [24]. Here, only the relevant changes are reported. First, there is now the possibility of directly scoring the STPR of any media, described in detail in section 2.4. Apart from this, raster scan files generated by the treatment planning software TRiP [25,26] can now be read by SHIELD-HIT in order to recalculate SOBPs. In this study, we present calculations from four single field carbon ion SOBPs, listed in Table 1. The width of the SOBP is defined as usual by the width in which the dose is above 95% percent [1]. All SOBPs are 3-dimensional dose cubes with equal side lengths. The resulting raster-scan file describes the needed amount of particles for each raster point and for each energy slice providing the necessary input for SHIELD-HIT to generate the radiation field for the SOBP. A ripple filter implementation based on the design described by Weber *et al.* [27] is added to SHIELD-HIT in a similar way as specified by Bassler *et al.* in [28], in order to produce flat SOBPs.

The practical range,  $R_p$ , is defined for protons as the depth at which the absorbed dose beyond the Bragg peak or SOBP falls to 10% of its maximum value [1]. However, for ions heavier than protons this definition of  $R_p$  is not feasible due to the pronounced dose tail of secondary particles. Therefore, the depth at which the absorbed dose beyond the Bragg peak or SOBP decreases to 50% of its maximum value is proposed and used here for ions heavier than hydrogen, i.e.,  $z > 1$ . Also other definitions of  $R_p$  have been used before as discussed in [29]. The residual range  $R_{\text{res}}$  at a depth  $d$  is then defined as

$$R_{\text{res}} = R_p - d \quad (2)$$

and the measurement depth  $d_{\text{ref}}$  at the middle of the SOBP in accord with TRS-398 [1].

### 2.1. Stopping powers and mean excitation energy

Stopping power  $S$  is defined as the average energy change  $dE$  of a particle per unit length  $dl$  in a medium. At high energies, that is about from 10 MeV/u up to 1 GeV/u,§ the mean energy loss of a charged particle to atomic electrons is well approximated by Bethe's original theory [30,31] which treats the electromagnetic interaction in first-order quantum perturbation theory. At lower energies, however, additional higher-order terms are required in order to reproduce experimental results. The transition from the regime of quantum perturbation theory to the one permitting a classical treatment is described in Bohr's distinguished survey paper [32].

A widespread formulation of Bethe's theory summarizing all terms of the lowest-order stopping number  $L_0$  was proposed by Fano [33]

$$\frac{S}{\rho} = \frac{4\pi e^4}{m_e v^2} \frac{1}{u} \frac{Z}{A} z^2 \left[ \ln \frac{2m_e v^2}{I} + \ln \frac{1}{1 - \beta^2} - \beta^2 - \frac{C}{Z} - \frac{\delta}{2} \right], \quad (3)$$

In Eq. (3),  $\rho$  is the density of the medium,  $m_e$  the electron mass,  $e$  and  $u$  are the elemental units of electric charge and atomic mass, respectively,  $Z$  and  $A$  are the atomic number and the relative atomic mass of the target medium, respectively,  $v$  and  $z$  are the velocity and the charge of the projectile, and  $\beta = v/c$  where  $c$  is the velocity of light in vacuum. The mean excitation energy of the target medium is denoted by  $I$ , while  $C/Z$  and  $\delta/2$  are the shell corrections and the density-effect correction, respectively. The second and third term in the square brackets containing  $\beta$  originate from Bethe's relativistic extension [31] and are often referred to as relativistic corrections. The expression in Eq. (3) is consistent with the first term  $L_0$  of the stopping number  $L$  in ICRU report 49 [17]. For low energies the description of the stopping powers becomes more complicated and higher-order terms of the stopping number  $L$  have to be taken into account in order to correct for a number of different effects, such as the Barkas and the Bloch correction,  $L_1$  and  $L_2$ , respectively. An effective description for the energy regime below the stopping-power maximum was provided by Lindhard and Scharff [34] assuming a rise of the stopping power which is proportional to the square root of the particle energy.

§ The energy regime from 10 MeV/u up to 1 GeV/u, corresponds according to the revised tables for water in ICRU 73 [6], for carbon ions to a range from 0.0427 cm up to 108.6 cm.

**Table 1.** Specifications of four spread out Bragg peaks (SOBPs) for carbon ions in water. Given are the width along the beam axis, the practical range  $R_p$ , and whether the SOBP is optimized for a homogeneous physical dose or relative biological dose. The optimization was performed by the treatment planning program TRiP [25, 26].

SOBP	Width (mm)	$R_p$ (mm)	Optimization
<i>a</i>	50	220	physical
<i>b</i>	80	168	physical
<i>c</i>	50	150	physical
<i>d</i>	100	153	biological

**Table 2.** Specifications for 6 sets of stopping-power data used in this work. The stopping-power data for the first three sets are determined internally by SHIELD-HIT (cf. Sec. 2.2) using the given values for  $I_{\text{water}}$  and  $I_{\text{air}}$ , while those for the sets 4 to 6 are directly read by SHIELD-HIT as text files in tabulated form. For the latter, two different tables per set are used distinguishing between the lightest (H and He) and heavier ions. The table specifies for each set its number,  $I_{\text{water}}$  and  $I_{\text{air}}$  in eV, the range of ions for which these data are applied, references, and if adequate additional comments. Further explanations can be found in the text.

SHIELD-HIT calculates stopping-power data using $I$ -values					
Set #	$I_{\text{water}}$	$I_{\text{air}}$	ion range	Reference	Comments
1	78	82.8	$z \geq 1$	ICRU 73 [6, 36]	using revised $I_{\text{water}}$ [36]
2	75	85.7	$z \geq 1$	ICRU 49 [17]	
3	80.8	85.7	$z \geq 1$	Henkner <i>et al.</i> [3]	
SHIELD-HIT directly uses tabulated stopping-power data					
Set #	$I_{\text{water}}$	$I_{\text{air}}$	ion range	Reference	Comments
4	78	82.8	$z > 2$	ICRU 73 [6, 36]	revised data for water [36]
	75	85.7	$z \leq 2$	ICRU 49 [17]	
5	67.2	82.8	$z > 2$	ICRU 73 [6]	only original data for water
	75	85.7	$z \leq 2$	ICRU 49 [17]	
6	75	85.7	$z = 1$	ICRU 49 [17]	charge scaling of ICRU 49
	75	85.7	$z > 1$	MSTAR [37]	

The mean excitation energy,  $I$ , is a property of the medium which enters logarithmically in the stopping formula Eq. (3), and is responsible for most of the target material dependence of the stopping-power. It is, on the other hand, completely independent of the properties of the projectile. According to Eq. (3), a larger  $I$ -value results in a smaller stopping power and consequently in a larger range of an ion in the medium. The  $I$ -values in the ICRU report 49 [17] for protons and alpha particles (retained from ICRU report 37 for electrons [35]) were mainly taken from measurements. In ICRU report 73 [6], however, the  $I$ -values are mostly determined theoretically. As a result different  $I$ -values for the same material are recommended in ICRU reports 49 and 73. Obviously, this is inconsistent, since an  $I$ -value should not depend on the projectile. The differences existing between the ICRU reports highlight that the accuracy of the current employed methods to determine stopping-power data have still to be improved in order to provide a consistent target description.

## 2.2. Stopping powers in SHIELD-HIT

In the current implementation of SHIELD-HIT the compilation of required stopping-power data can be done in two ways which can be chosen independently for each target

medium. First, stopping-power data can be calculated internally by SHIELD-HIT using a modified Bethe formula at high energies and a Lindhard-Scharff description [34] at low energies for any kind of material composition using the corresponding material-specific values for  $I$ ,  $Z$ , and  $A$  as discussed before in Sec. 2.1. Second, an arbitrary stopping-power table may be read in as a formatted text file allowing for the use of, in principle, any stopping-power data which can be provided in electronic form. In this work the common open source library *libdEdx* [38, 39] which is available online is applied in order to provide tabulated data in formatted form from the ICRU reports 49 [17, 40] and 73 [6, 36] as well as MSTAR [37].

The Bethe formula used by SHIELD-HIT is similar to the formulation in Eq. (3). But, so far no shell corrections  $C/Z$  have been considered. These are known to be most relevant for low energies where, however, the Lindhard-Scharff description is used instead in SHIELD-HIT. Furthermore, it was demonstrated that for low energies (about 1 MeV/u) the accuracy of stopping-power data is insignificant for particle therapy [41]. The same argument holds for the higher-order term  $L_1$ . Additionally, the Bethe formula is modified in order to allow for electron capture (significant for low energies) by using an effective energy-dependent scaling of the projectile charge  $z$  by Hubert *et al.* [42]. Currently, relativistic corrections proposed by Lindhard and Sørensen [43] are still missing in SHIELD-HIT. Their importance increases for heavy ions with large nuclei which cannot be approximated as point-like particles. Although their relevance for particle therapy should be studied no significant impact has been expected so far.

Due to existing inconsistencies in the stopping-power data recommended by ICRU — discussed in Sec. 2.1 — different sets of stopping powers are used in this work, all listed in Table 2. Thereby, sets 1 and 2 as well as sets 4 and 5 are directly related to ICRU reports. For comparison, in set 3 the preferred  $I$ -values of Henkner *et al.* [3] are used while set 6 employs the frequently used data provided by MSTAR [37]. The intended purpose of the sets 1 and 2 is the attempt to describe the target media consistently with only one  $I$ -value for all ions, both with  $z \leq 2$  as well as  $z > 2$ , applying SHIELD-HIT's internal routine to determine the stopping power. Accordingly, set 1 uses only the  $I$ -values from ICRU report 73,  $I_{73}$ , (the revised value for water,  $I_{\text{water}} = 78$  eV, was very recently published in the erratum to ICRU 73 [36]) while only  $I$ -values from ICRU 49,  $I_{49}$  are used in set 2. The motivation for sets 4 and 5, on the other hand, is the direct application of the recommended tabulated data which can be found in ICRU reports 49 and 73 for ions with  $z \leq 2$  and  $z > 2$ , respectively. While set 4 uses the recently revised stopping-power data for heavy-ions on water, set 5 uses, for comparison to earlier studies of the STPR, the water data as originally published in ICRU 73. Note, the recently revised data from ICRU 73 [36] were not employed by Henkner *et al.* [3].

### 2.3. Stopping-power ratio

The stopping-power ratio  $S_{a/b}$  between medium  $a$  and medium  $b$  is (cf. TRS-398|| [1]) given as a particle fluence weighted average over all primary and secondary particles. It is determined by calculating the dose ratio via track-length fluence  $\Phi_{a,i}(E)$  of particle  $i$  in medium  $a$  as function of particle energy  $E$  and mass stopping power  $S_i(E)/\rho$

$$S_{a/b} = \frac{\sum_i \int_{E_{\min}}^{\infty} \Phi_{a,i}(E) (S_i(E)/\rho)_a dE}{\sum_i \int_{E_{\min}}^{\infty} \Phi_{a,i}(E) (S_i(E)/\rho)_b dE}. \quad (4)$$

In Eq. (4) numerator and denominator are equal except for that the mass stopping power of medium  $a$  enters in the numerator and of medium  $b$  in the denominator. An energy cutoff  $E_{\min} > 0$  may originate, e.g., from the chamber geometry. The contribution of “track-ends” to the total dose deposition and to the corresponding STPR was studied in [44]. There it was concluded that they are not of relevance for light-ion dosimetry which is in contrast to electrons, where the contribution to the total deposited dose can be between 6% and 8% [35].

In contrast to the correct definition for the STPR of an ion field in Eq. (4), the *ratio of stopping powers* for media  $a$  and  $b$  for one particle species of energy  $E$ ,

$$\frac{(S(E)/\rho)_a}{(S(E)/\rho)_b} = \frac{\langle \frac{Z}{A} \rangle_a \ln[2m_e v^2/I_a]}{\langle \frac{Z}{A} \rangle_b \ln[2m_e v^2/I_b]}, \quad (5)$$

has often been considered as an approximation to the STPR, e.g. in [1, 3, 4]. The right hand side of Eq. (5) is expressed by Bethe’s stopping formula as given in Eq. (3) but omitting corrections. Note, the ratio in Eq. (5), which considers only one particle species, is a function of the particle *energy*  $E$  in contrast to the STPR in Eq. (4) which has a *spatial* dependence and takes the full energy spectra of all particles into account.

### 2.4. Scoring of STPR in SHIELD-HIT

STPRs have already been obtained with SHIELD-HIT before [3, 5] and only the conceptual improvements in this work are discussed in the following. The concept of virtual scoring has been introduced which now allows for a parallel detector geometry independent of any physical geometry. Therefore, there is no longer a need for introducing artificial physical geometries which lead to additional region boundaries. Furthermore, the STPRs are now determined *on-line*, that is, during the transport of the particles. An on-line calculation has the advantage that possible influence on the result due to the number and size of the energy scoring and energy spacing is avoided. Additionally, higher accuracy in scoring of tracks-ends can be achieved in principle.

The detector for the STPR resembles Eq. (4) and is implemented in the following way. When a particle traverses a bin of the STPR detector its track-length fluence within the bin is scored and directly multiplied with  $(S/\rho)_a$  of the medium  $a$  in which

|| In IAEA TRS-398 only the water-to-air STPR is explicitly defined, i.e.,  $a$ =water and  $b$ =air. However, this definition is also useful for other media combinations.



the particle moves for the energy  $(E_{\text{in}} + E_{\text{out}})/2$ .  $E_{\text{in}}$  and  $E_{\text{out}}$  are the energies of the particle when it enters and leaves the bin, respectively. Additionally, the *same* track-length fluence is multiplied with  $(S/\rho)_b$  of the same particle. Both quantities are summed up individually including all particles passing the bin. After a full Monte Carlo transport simulation the two sums are divided yielding the STPR for this bin.

In this work a transport cutoff of 0.025 MeV/u is used by SHIELD-HIT which means that all particle tracks end once the particle energy becomes smaller.¶ Consequently, the lower limit for the integration in Eq. (4) is given by  $E_{\text{min}} = 0.025$  MeV/u having an influence on the STPR of less than 0.00015% [3]. A recent review article [45] discusses in some detail the impact of electrons in fast ion-atom collisions with respect to hadron therapy as well as the possibility to extend SHIELD-HIT in a way that also electron tracks are considered. This would allow for studies of the microscopic energy distribution in the target medium. Tracking of delta-electrons has for example been performed with Geant4 [46] and a study comparing to the present work might be of interest.

### 2.5. Analytic expression for the average ion energy

The stopping-power formula as presented in Eq. (3) for a specified combination of projectile and target is primarily a function of the projectile's kinetic energy which decreases during the passage through the target medium due to the energy loss. In order to determine the average energy of the projectiles as a function of depth a full simulation of the particle transport has to be performed. This comprises the slowing down caused by all relevant energy-loss mechanisms including elastic as well as nonelastic interactions [47]. Thereby, nonelastic nuclear reactions produce a spectrum of particles with each particle having an individual energy distribution which is furthermore a function of the position in the medium. Consequently, it would be highly desirable to have a simple, though approximate, analytical expression  $E(d)$  for the average energy of the primary particles with initial energy  $E_0$  as function of penetration depth  $d$ .

Starting with the Bethe formula, but assuming first that the expression in the square brackets of Eq. (3) is independent of energy,  $E(d)$  can easily be expressed analytically,

$$E(d; E_0, R_p) \approx E_0 \left( 1 - \frac{d}{R_p} \right)^{1/2}, \quad (6)$$

where  $R_p$  is the practical range.  $R_p$  depends in general on the ion species,  $E_0$ , and the target material. For energies relevant in particle therapy  $R_p$  can often be approximated by  $R_0$  obtained with the continuous slowing down approximation (CSDA).

In order to account for the correct energy dependence of the Bethe formula as well as nonelastic collisions one has to allow for a more general power-law relation,

$$E(d; E_0, R_p) = E_0 \left( 1 - \frac{d}{R_p} \right)^{1/k}, \quad (7)$$

¶ This is consistent with ICRU 73 [6] where the range tables for liquid water show the average path length travelled for slowing-down from initial energy  $E$  to  $E_0 = 0.025$  MeV/u.

with an exponent  $k$ . Different values for  $k$  are suggested in the literature while Kempe and Brahme [29] proposed the use of a dimensionless transport parameter  $k = E_0/R_0S_0$  with  $S_0 = S(E_0)$ . A simple value of about  $k = 1.7$  fits the calculations performed with SHIELD-HIT being also compatible with [29] and is therefore used in this study.

### 2.6. Analytic expression for STPR

In order to derive an analytic, though approximate, expression of the STPR as a function of the depth  $d$  for two media  $a$  and  $b$ , the approximation to the average energy in Eq. (7) can be used together with the ratio of stopping powers given in Eq. (5). Utilizing the non-relativistic relation  $v^2 = 2E/m_p$  between the particle velocity  $v$  and its kinetic energy  $E$ , where  $m_p$  is the proton mass, one obtains the expression

$$\tilde{S}_{(a/b)}(d) = \frac{\langle \frac{Z}{A} \rangle_a \ln[E_0/I_a] + C(d)}{\langle \frac{Z}{A} \rangle_b \ln[E_0/I_b] + C(d)} \quad (8)$$

where

$$C(d) = \frac{1}{k} \ln \left[ 1 - \frac{d}{R_p} \right] - 6.1291 \quad (9)$$

and  $\ln[4m_e/m_p] = -6.1291$  have been used. Similar as in Eq. (4) the numerator and denominator in Eq. (8) equal except for the different  $I$ -values and  $\langle Z/A \rangle$  ratios. It should be mentioned that in order to keep the expression for  $\tilde{S}_{(a/b)}$  as simple as possible its derivation has been performed without relativistic kinematics which are in principal of relevance for the highest energies used in particle therapy. Finally, the expression in Eq. (8) should explicitly be formulated for the water-to-air STPR

$$\tilde{S}_{(\text{water/air})}(d) = 1.11195 \frac{\ln[E_0/I_{\text{water}}] + 1/k \ln [1 - d/R_p] + 7.6863}{\ln[E_0/I_{\text{air}}] + 1/k \ln [1 - d/R_p] + 7.6863}, \quad (10)$$

being the most relevant case for dosimetry in particle therapy, with  $E_0$  and  $I$  in units of MeV/u and eV, respectively. For convenience, constants are expressed in numbers, i.e.,  $\ln[4 \times 10^6 m_e/m_p] = 7.6863$  and  $\langle \frac{Z}{A} \rangle_{\text{water}} / \langle \frac{Z}{A} \rangle_{\text{air}} = 0.555076 / 0.499189 = 1.11195$  [35].

## 3. Results

In what follows, results for STPRs of pristine Bragg peaks and SOBPs are presented. Furthermore, analytic expressions are compared to the numerical results obtained with SHIELD-HIT. For simplicity, only results for ion beams in water are considered, and STPRs are presented exclusively for water-to-air. Furthermore, only stopping-power set 1 of Table 2 is used in order to ensure consistent results except for Fig. 1(b) which demonstrates the dependence of  $S_{\text{water/air}}$  on the choice of the stopping-power set.

### 3.1. Pristine Bragg peaks

A comparison between the calculated STPR for water-to-air of 270 MeV/u carbon ions as a function of depth in water and the corresponding depth-dose distribution is shown

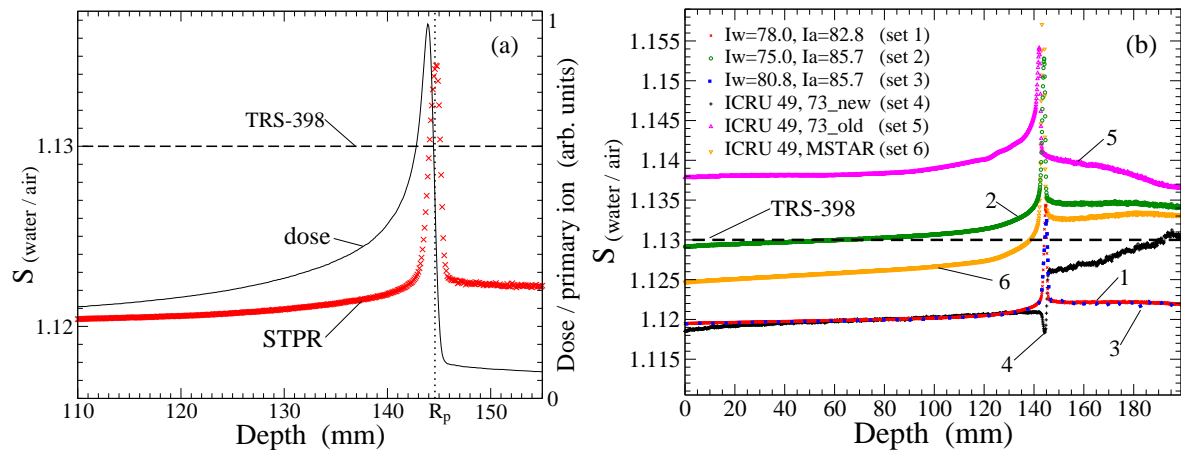


**Figure 1.** 270 MeV/u carbon ion beam in water. (a) Depth-dose distribution (line) and stopping-power ratio  $S_{\text{water/air}}$  (symbol) as a function of depth around the Bragg peak. The stopping-power set 1 is used. (b)  $S_{\text{water/air}}$  as function of depth obtained with the six stopping-power sets 1–6 as specified in Table 2 and the value 1.13 recommended by IAEA in TRS-398 [1].

in Fig. 1(a) focusing on the vicinity of the Bragg peak. The maximum of the STPR almost coincides with the practical range  $R_p = 144.6$  mm and therefore appears to be at a larger depth than the dose maximum. The width of the STPR peak is considerably smaller than that of the dose curve. The determined height of the STPR depends to some extent on the finite spatial resolution along the beam axis. A coarse resolution leads to spatial averaging and accordingly to a lower peak height of the STPR. Note, the position of the Bragg peak and therefore  $R_p$  is only influenced by the choice of stopping-power data for water.

The influence on the STPR due to the use of different stopping-power data is demonstrated in Fig. 1(b) for a 270 MeV/u carbon pencil beam by using all stopping-power sets 1 to 6 of Table 2. In the plateau region, the deviations of the sets 1 to 6 from the value 1.13 recommended by the IAEA in the TRS-398 [1] is within 1%. Set 2, which employs  $I_{49}$  for water and air, differs the least. This is consistent since the recommendation in TRS-398 is based on the stopping-power data provided by ICRU report 49. In contrast to the recommended value 1.13, none of the calculated STPR curves is constant. However, the relative increase in the plateau region up to a depth of 130 mm ( $R_{\text{res}} \approx 15$  mm) is moderate and of the order of approximately 0.2% to 0.3%. For all sets of stopping powers, except for set 4, an increase of the STPR can be observed in the vicinity of the Bragg peak. Set 4 on the other hand shows a dip. This dip originates mostly from the carbon ions and can therefore be attributed to the tabulated data provided by in the revision of ICRU 73.

The two STPR curves calculated with set 1 and set 3 — the latter was used in [3] — lie virtually on top of each other in Fig. 1(b) although the  $I$ -values of set 1 and set 3 differ notably. This can be explained by the differences of the  $I$ -values for water and air which are very similar with 4.8 eV and 4.9 eV for set 1 and set 3, respectively. As

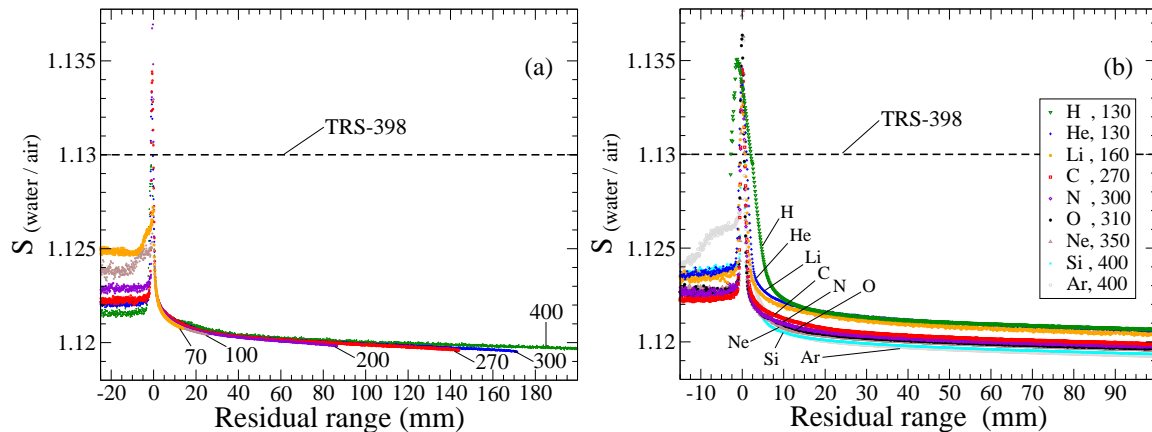


**Figure 2.** Stopping-power ratio for water-to-air  $S_{\text{water/air}}$  as a function of  $R_{\text{res}}$  in water. The stopping-power set 1 specified in Table 2 is used. (a) Carbon ions with different initial energies ranging from 70 MeV/u to 400 MeV/u are compared. (b) Beams of different ions relevant for particle therapy are compared: H, He, Li, C, N, O, Ne, Si, and Ar. Ion beam energies ranging from 130 MeV/u to 400 MeV/u have been chosen in order to achieve comparable penetration depths.

expected, the  $S_{\text{water/air}}$  obtained with the tabulated data from ICRU 73, that is set 4, agrees with the STPR curve obtained with  $I_{73}$ , set 1, in the plateau region. On the other hand, the STPR curves for the sets 1 and 4 deviate around and beyond  $R_p$ . The use of the stopping-power set 5 by Henkner *et al.* in [3] resulted in an unphysical minimum of the STPR in the plateau region. In the present study, however, no minimum of the  $S_{\text{water/air}}$  curve obtained with set 5 can be observed.

The influence of different initial energies on the STPR for carbon ion beams as function of the residual range  $R_{\text{res}}$  is shown in Fig. 2(a). The STPR curves as function of  $R_{\text{res}}$  are almost identical in the plateau region and therefore independent of the initial energy. Around and beyond the Bragg peak the curves are still alike, though lower initial energies lead in general to higher STPRs values.

Stopping-power ratio  $S_{\text{water/air}}$  as a function of  $R_{\text{res}}$  for different ion beams relevant for particle therapy: H, He, Li, C, N, O, Ne, Si, and Ar are presented in Fig. 2(b). Different beam energies for the individual ions have been chosen, ranging from 130 MeV/u to 400 MeV/u, in order to achieve comparable penetration depths. In the plateau region the STPRs for the different ion beams all share the same qualitative behavior which has already been discussed before in the context of carbon ions, cf. Figs. 1(b) and 2(a). A comparison among the ions yields that decreasing STPRs at a given  $R_{\text{res}}$  occur for increasing atomic numbers  $z$ . The decrease becomes less pronounced for larger  $z$ . An exception from this trend is found for H and He ions with very similar  $S_{\text{water/air}}$  in the plateau. The relative difference of STPRs between the lightest and heaviest ion  $z = 1$  and  $z = 18$ , respectively, is rather constantly about 0.15%.

Around and beyond  $R_p$  ( $R_{\text{res}} \lesssim 0$ ), the STPR seems to be larger for ions with larger  $z$ . Although, some dependence also might originate from the different initial energies of the ion beams, as has been observed in Fig. 2(a). While the STPR for H ions is

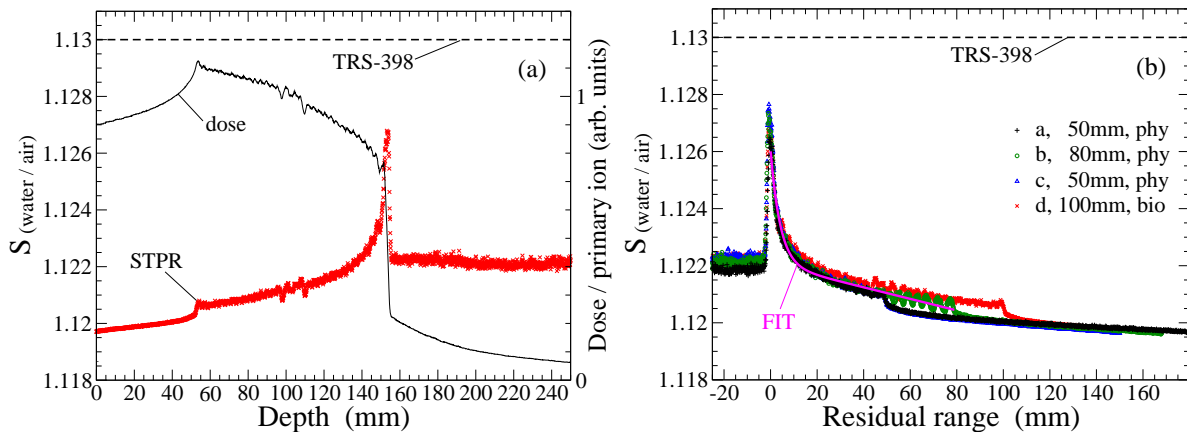


**Figure 3.** Different SOBPs for carbon ions in water as specified in Table 1. The stopping-power set 1 specified in Table 2 is used. (a) Depth-dose distributions (line) and STPRs  $S_{\text{water/air}}$  (symbol) as a function of depth for the biologically optimized SOBP *d*. (b) STPRs  $S_{\text{water/air}}$  as a function of the residual range  $R_{\text{res}}$  for all four SOBPs *a*, *b*, *c*, and *d*. Also shown is a simple fit for set 1 proposed in Eq. (11).

nearly identical to that for He ions in the plateau region, differences to all other ions with  $z > 1$  are obvious for  $R_{\text{res}} \lesssim 0$ . However, as discussed in Sec. 2, the definition of the practical range  $R_p$  for protons differs from that used for ions with  $z > 1$  which influences — according to Eq. (2) — also the residual range  $R_{\text{res}}$ .

### 3.2. Spread-out Bragg peaks

Four different SOBPs obtained with carbon ion fields are considered with the stopping-power set 1 in this study and their properties are listed in Table 1. Figure 3(a) displays the depth-dose distribution (line) and the corresponding STPR (symbol) of the biologically optimized SOBP *d*. The proximal start of the SOBP region can be recognized in STPR curve as a significant increase. Towards the distal end of the SOBP the STPR reveals an exponential increase. As for pristine peaks in Fig. 1(a) the maximum of the STPR curve is reached close to  $R_p$ . A sharp fall off of the STPR occurs for depths  $d > R_p$  which finally results in a constant STPR. Note, this qualitative description is valid for all SOBPs *a* to *d* and is therefore independent of the specific form of the SOBP or whether it is physically or biologically optimized.

The STPRs of all four SOBPs *a*, *b*, *c*, and *d* are compared in Fig. 3(b) as a function of  $R_{\text{res}}$ . The SOBPs *a* and *c* share the same width but differ in  $R_p$ . Therefore, their STPRs as a function of  $R_{\text{res}}$  are nearly identical. The STPR curves for *b* and *d* show a very similar behavior as *a* and *c* but are extended to 80 mm and 100 mm, respectively, according to the larger width of their SOBP region.

It should be mentioned that for SOBP *b* a number of ripples in the STPR can be observed in the proximal SOBP region. They originate from the optimization program TRiP which assumes treatment at the SIS accelerator at Gesellschaft für Schwerionenforschung (GSI), Darmstadt, Germany. The SIS provides finite energy steps

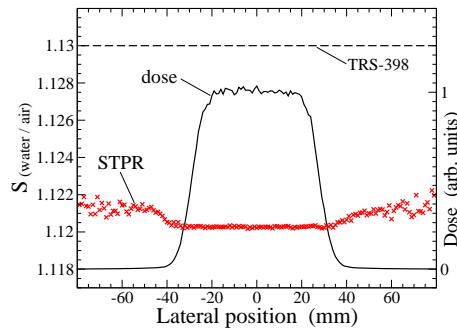


**Figure 4.** SOBP  $c$  for carbon ions in water as specified in Table 1. The stopping-power set 1 specified in Table 2 is used. Dose distribution (line) and STPR  $S_{\text{water/air}}$  (symbol) as a function of transverse position at a depth  $d_{\text{ref}} = 150$  mm.

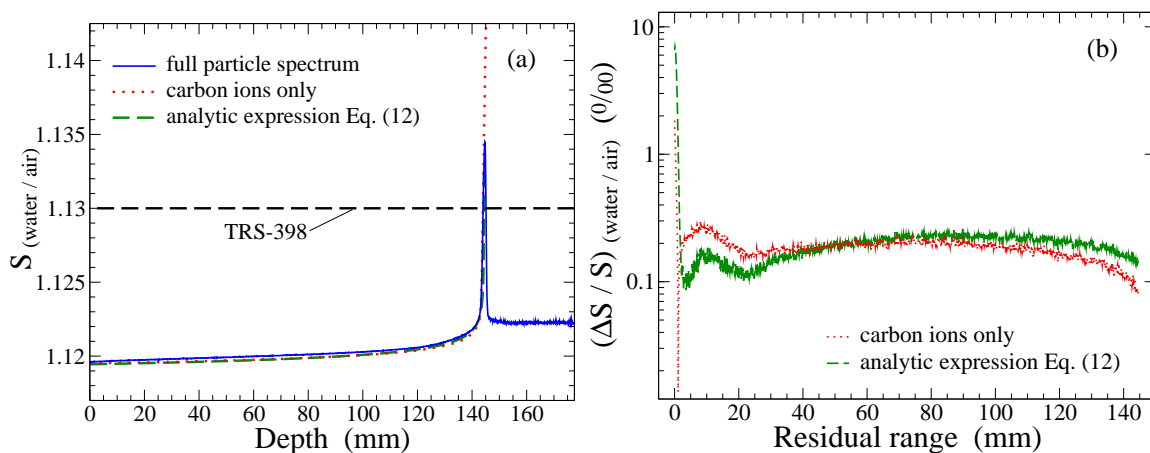


**Figure 5.** Stopping-power ratio  $S_{\text{water/air}}$  for a 270 MeV/u carbon ion beam in water. The stopping-power set 1 specified in Table 2 is used. The STPR obtained with the full particle spectrum is compared to two different approximations: STPR determined (i) by considering only the contribution from carbon ions, and (ii) with the analytic expression proposed in Eq. (10). (a) Absolute  $S_{\text{water/air}}$  as a function of depth. (b) Relative difference between the STPR for the full particle spectrum and the two approximations to the STPRs presented in (a) as a function of residual range.

which are more coarse at the lowest energy part when no bolus is applied.

The calculated STPR and dose transverse to the beam axis at the reference depth  $d_{\text{ref}} = 150$  mm (defined as middle of SOBP [1]) is displayed in Fig. 4 for the SOBP  $c$ . The STPR is perfectly constant within the full extension of the SOBP transverse to the beam axis. A moderate increase of the STPR occurs outside the SOBP.

### 3.3. Analytical description of STPR

The purpose of this section is to relate an analytical description of the STPR to the numerically obtained STPR. Thereby, it is important to keep in mind that according to the results obtained so far the STPR (a) depends primarily on  $R_{\text{res}}$ , that is average ion energy, and (b) is qualitatively independent of the ion species.

The STPR  $S_{\text{water/air}}$  for a 270 MeV/u carbon ion beam using the stopping-power set 1, as shown before in Fig. 1(b), which considers the full particle spectrum is compared in Fig. 5 to two approximations of the STPR: (i) STPR obtained with SHIELD-HIT but ignoring the influence of produced fragments on  $S_{\text{water/air}}$  by only considering the STPR resulting from carbon ions and (ii) the analytic expression in Eq. (10) which approximates the STPR with a ratio of stopping powers of the primary ions with an average energy depending on  $R_{\text{res}}$ . Figure 5(a) clearly shows that especially in the plateau region the absolute difference between these three curves is small. Therefore, Fig. 5(b) additionally shows the relative difference  $|S^{\text{full}} - S^{\text{appr}}| / S^{\text{full}}$  between the STPR for the *full* particle spectrum, determined according to Eq. (4), and the two approximations of the STPR. Both approximations reproduce  $S^{\text{full}}$  within 0.02% in the whole plateau region. Around  $R_p$  the difference can be as large as 1% and they cannot be applied beyond  $R_p$  since both approximations are based on the primary particles.

In principle, the analytical expression for pristine peaks can also be of use for SOBP. However, since the exact weights of the superposed peaks are not always known a simple fit as a function of  $d$  may be proposed

$$S_{\text{water/air}}(d) = \alpha + \beta \exp[\gamma(R_p - d)] + \delta (R_p - d) \quad (11)$$

which approximates the STPR within the SOBP region and is also shown in Fig. 3(b). The values for the four parameters in Eq. (11) are

$$\alpha = 1.12205, \quad \beta = 4.0044\text{E-}03, \quad \gamma = -0.241, \quad \text{and} \quad \delta = -2.0238\text{E-}05.$$

These parameters depend on the stopping-power set and slightly on the ion species [39]. Outside the SOBP region the STPR might be approximated in a similar way as it is done for pristine peaks considering the average energy of the primary ions at  $d$  which is, however, different from the case of pristine peaks. From Fig. 3(b) it can be observed that the fit function proposed in Eq. (11) clearly is in acceptable agreement with the  $S_{\text{water/air}}$  curves of the four different SOBPs.

## 4. Discussion

### 4.1. Influence of the inconsistency of ICRU stopping-power data on the STPR

It is obvious that the STPR strongly depends on the stopping-power data which are used as an input for its determination. This applies for  $R_p$  and accordingly the position of the STPR maximum. Therefore, the present work focuses mainly on stopping-power data for water and air which are recommended by ICRU reports. However, even if one tries to follow these recommendations certain inconsistencies still remain and different sets of stopping-power data — as listed in Table 2 — can be deduced. In the case that the tabulated data provided by ICRU are used directly, set 4, physical quantities of the target media, e.g., the  $I$ -value are depended on whether the medium interacts with protons and helium ions or with heavier ions. Although not explicitly recommended, another approach, which is more consistent from a physical point of view, is to use the  $I$ -values of only one of the ICRU reports together with an appropriate stopping formula

for all ions, i.e., with  $z \leq 2$  as well as  $z > 2$ . This is done here for set 1 and set 2 using  $I_{73}$  and  $I_{49}$ , respectively.<sup>+</sup>

First, the STPRs in the plateau region ( $d < R_p$ ) are discussed. Figure 1(b) reveals that the STPR  $S_{\text{water/air}}$  using  $I_{49}$  for all ions, set 2, agrees best with a constant value of 1.13 as recommended in TRS-398 which is plausible since TRS-398 is based on the data of ICRU 49.  $S_{\text{water/air}}$  obtained with  $I_{73}$ , set 1, is about 1% smaller compared to that obtained with  $I_{49}$ , set 2 but agrees nicely with the tabulated data recommended by ICRU, set 4. Second, around  $R_p$  the STPR curves of all data sets show a distinct maximum except for that of set 4 for which a minimum can be observed. This minimum does not originate from differences in the target descriptions due to the use of ICRU 49 and 73 in set 4 but is exclusively caused by the low-energy ratio of stopping powers taken from ICRU 73. Third, beyond the peak ( $d > R_p$ )  $S_{\text{water/air}}$  is rather constant for all stopping-power sets with a consistent description of the target media. For set 4 and set 5 the faster decline of the heavier ions relative to the lighter ones beyond  $R_p$  leading to a transition from ICRU 73 to 49 is clearly revealed by 1(b). Therein, the latter two curves finally converge to  $S_{\text{water/air}}$  obtained with  $I_{49}$ , set 2.

The use of the out-dated standard, that is stopping tables from ICRU 49 and 73 *without* the revisions of ICRU 73 for water, set 5, is not advised. Set 5 yields a STPR which is in the plateau region about 1% and 2% larger than the value 1.13 recommended by TRS-398 and the values obtained *with* revisions of ICRU 73 for water, set 4, respectively. It should be mentioned, that the results for set 5 in Fig. 1(b) do not show any unphysical minimum in the plateau region as was observed before in [3, 4]. There, the unphysical structure was attributed to the use of different stopping-power data from ICRU 49 and 73 for different ions. However, in the present work it was possible to reproduce the exact shape of the curve as shown in Fig. 2 of [3] by using only three digits of the stopping-power data of ICRU 49 and 73 instead of the four digits provided by the tables and therefore to contradict the earlier statement. We can conclude that the reason for the unexpected behavior observed in the corresponding Fig. 2 of [3] is simply due to errors resulting from a too coarse rounding in the applied stopping-power list and are not caused by a combined use of ICRU 49 as well as 73.

#### 4.2. Dependence of the STPR on the average ion energy

One quintessence of this work is that the STPR for a given set of stopping-power data is mostly determined by the average energy of the ions, rather than their initial energy or their charge which is nicely confirmed by Fig. 2 Figure 5 shows furthermore that for  $d < R_p$  the STPR is completely dominated by the STPR of the primary ion species and the

<sup>+</sup> A further option is to correct for the  $I$ -value in one of the two recommended sets of ICRU tables leading to a more consistent description of the target media. According to Eqs. (3) this could be done in first order using the term  $0.307075 (z^2 Z) / (\beta^2 A) \ln[I_{49}/I_{73}]$  for correcting ICRU report 49 or its negative value for correcting ICRU report 73 [48]. This approach is of course not applicable in the low-energy regime where, on the other hand, the ICRU tables anyhow provide a limited accuracy only. However, this option has not been pursued in this work.



relative deviation is of the order of 0.02%. In a next step, the STPR of the primary ions can be nearly exactly reproduced using the ratio of stopping powers, as expressed in Eq. (5), for the average energy of the primary ions at a depth  $d$ . Since the average energy can be rather accurately expressed as a function of  $d$ , in a final step this energy function is used together with Eq. (5) to formulate the analytical expression of the STPR in Eq. (10). The analytical expression reproduces the STPR of the primary ions very well and deviates accordingly also in the order of 0.02% from the correct STPR obtained with the complete particle spectrum.

Note, the key advantage of the proposed analytical expression is its flexibility. It is not restricted to a specific set of stopping-power data. Consequently, it could be easily adopted to any new recommendation by ICRU. It is not restricted to specific primary ions and only their average energy as a function of depth is required. It is not restricted to a specific combination of target materials such as water and air being in the focus of the present work. For example, it can be straightaway used for STPR for water to tissue and air to tissue which would be of interest when comparing dose to medium with dose to water as recently discussed by Paganetti [49].

These findings lead to two central insights. First, in contrast to the presumption in TRS-398, the knowledge of the whole particle spectra is not of practical importance for the plateau and peak region.\* The STPR can be simply approximated with a relative deviation much smaller than the uncertainties of all available stopping-power data. On the other hand, the secondary particles are of central importance beyond  $R_p$  where the primary ions are ceased. Second, it is not necessary to study STPRs for all ions independently since they can be approximated in the same way as proposed in Eq. (8). The small quantitative differences among the STPRs of the various ions shown in Fig. 2(b) may be explained best with the different average energies at a given  $R_{\text{res}}$ .

#### 4.3. STPRs for SOBPs

Clinical applications require a relatively uniform dose to be delivered to the volume to be treated and for this purpose the ion beam has to be spread out both laterally and in depth. With respect to the STPR of SOBPs the gist of this work is that the qualitative behavior of the STPR is hardly dependent on the specific spatial form of the SOBPs, its depth in the medium, and whether it is optimized for a homogeneous physical dose or relative biological dose.

This statement is nicely verified in Fig. 3(b) where  $S_{\text{water/air}}$  is displayed as a function of  $R_{\text{res}}$  for four SOBPs specified in Table 1. In order to understand the observed uniform behavior of the STPR one has to keep in mind that a SOBP is a superposition of Bragg peaks of different intensities and  $R_p$  which is usually constructed from the distal end, i.e.  $R_{\text{res}} = 0$ , toward the proximal start. Consequently, the properties of the SOBP up till a residual range  $R_{\text{res}}$  are only weakly influenced by the properties of the SOBP for larger

\* The relevance of the whole particle spectra for determining the STPR increases if for some secondary particles different stopping-power data are employed, e.g. ICRU 73 and 49.

$R_{\text{res}}$ . It is therefore possible and practical to propose a fit to the STPR  $S_{\text{water/air}}$  for the SOBP region, as it is done in Eq. (11) for carbon ions and set 1. A general drawback of the fit function compared to an analytical expression is that the parameters of the former explicitly depend on the ion species and stopping-power data. In analogy to the findings for pristine peaks quantitative differences can be expected for ion species other than carbon ions. However, a detailed study of a number of other ions is beyond the scope of this article and might be addressed elsewhere [39]. The qualitative dependence of  $S_{\text{water/air}}$  on the stopping-power set is similar as discussed before for the pristine peaks. Accordingly, the quantitative difference between  $S_{\text{water/air}}$  obtained with set 1 and set 4 is due to the two features observed for set 4, namely, the minimum at  $R_p$  and the strong increase of the STPR beyond  $R_p$  caused by the ICRU 49 tables for protons and helium.

In TRS-398 reference conditions for the determination of absorbed dose for ion beams are specified. The reference depth  $d_{\text{ref}}$  for calibration should be taken at the middle of the SOBP, at the center of the target volume. It can be seen in Fig. 4 that a positioning error of a dosimeter transverse to the beam axis has no relevance on the STPR as long as the position is within the SOBP. This is plausible since the average energy of the ions should be same at the same depth. A misalignment along the beam axis, on the other hand, may have an influence as seen in Fig. 3. The influence is largest for a SOBP with small width, for which the gradient of STPR is largest, and becomes smaller for large widths. Therefore, an extended SOBP might be recommended for accurate dose measurements in a practical quality-assurance setting. The total variation of the STPR along the beam axis observed in Fig. 3(b) is of the order of 0.8%.

## 5. Conclusions

Calculations of the water-to-air stopping-power ratio (STPR)  $S_{\text{water/air}}$  using the Monte Carlo transport code SHIELD-HIT10A are performed for different ions in a range of  $1 \leq z \leq 18$ . The STPR is determined on-line considering the track-length fluence spectra of all primary and secondary particles as recommended by IAEA in TRS-398. In addition to providing accurate quantitative results the focus of this work is put on a thorough qualitative understanding of the dependencies of the STPR and the relevance for particle therapy.

STPRs obtained with different sets of stopping-power data recommended by ICRU [6, 17], including the very recently revised data for water [36], are compared with the value 1.13 recommended for  $S_{\text{water/air}}$  in TRS-398 [1] resulting in deviations of the order of 1% in the plateau region. The change of the STPR due to the contribution of secondary particles is only of the order of 0.02% for pristine peaks in the plateau region and up to the Bragg peak. It can be shown that for a given set of stopping-power data the STPR at a residual range  $R_{\text{res}}$  is mostly determined by the average energy of the primary ions, rather than their initial energy or their charge  $z$ . A convenient analytical expression for the STPR as a function of depth in water is proposed for the plateau region up to the Bragg peak which deviates in this region by about 0.02% from the

obtained results for  $S_{\text{water/air}}$ . The most valuable property of the analytical formula is its flexibility. It is in principle not restricted to any specific ion, stopping-power data, combinations of target media, or initial ion energies. For the case of spread-out Bragg peaks (SOBPs) it can be concluded that the qualitative behavior of the STPR is hardly dependent on the specific spatial form of the SOBPs, its depth in the medium, and whether it provides a homogeneous physical dose or relative biological dose. A fit function is provided to approximate the STPR within the SOBPs region for carbon ions.

Finally, it can be stated that no further theoretical studies of STPRs heading only for higher accuracy are expedient, as long as no consistent set of relevant stopping-power data for all ions is recommended, preferably with smaller uncertainties.

## Acknowledgments

This work is supported by the Danish Cancer Society (<http://www.cancer.dk>), and the Lundbeck Foundation Centre for Interventional Research in Radiation Oncology (<http://www.cirro.dk>).

## References

- [1] IAEA TRS-398. Absorbed dose determination in external beam radiotherapy an international code of practice for dosimetry based on standards of absorbed dose to water. Technical report, International Atomic Energy Agency, 2000.
- [2] G. H. Hartmann, O. Jäkel, P. Heeg, C. P. Karger, and A. Krießbach. Determination of water absorbed dose in a carbon ion beam using thimble ionization chambers. *Phys. Med. Biol.*, 44(5):1193, 1999.
- [3] Katrin Henkner, Niels Bassler, Nikolai Sobolevsky, and Oliver Jäkel. Monte carlo simulations on the water-to-air stopping power ratio for carbon ion dosimetry. *Med. Phys.*, 36:1230, 2009.
- [4] Helmut Paul, Oksana Geithner, and Oliver Jäkel. The influence of stopping powers upon dosimetry for radiation therapy with energetic ions. volume 52 of *Advances in Quantum Chemistry*, pages 289 – 306. Academic Press, 2007.
- [5] O. Geithner, P. Andreo, N. Sobolevsky, G. Hartmann, and O. Jäkel. Calculation of stopping power ratios for carbon ion dosimetry. *Phys. Med. Biol.*, 51:2279–2292, 2006.
- [6] ICRU Report 73. Stopping of ions heavier than helium. *J. ICRU*, 5:1, 2005.
- [7] Helmut Paul. Recent results in stopping power for positive ions, and some critical comments. *Nucl. Instrum. Methods Phys. Res. B*, 268(22):3421 – 3425, 2010.
- [8] D. Schardt, P. Steidl, M. Krämer, U. Weber, K. Parodi, and S. Brons. Precision Bragg-curve measurements for light-ion beams in water. GSI Scientific Report 2007 2008-1. 373, GSI, 2008. Available from: <http://www.gsi.de/informationen/wti/library/scientificreport2007/PAPERS/RADIATION-BIOPHYSICS-19.pdf>.
- [9] S. Agostinelli et al. Geant4 - a simulation toolkit. *Nucl. Instrum. Methods Phys. Res. A*, 506(3):250–303, 2003.
- [10] A. Fassò, A. Ferrari, J. Ranft, and P. R. Sala. FLUKA: a multi-particle transport code. CERN-2005-10, INFN/TC\_05/11, SLAC-R-773, 2005.
- [11] H. Iwase, K. Niita, and T. Nakamura. Development of general-purpose Particle and Heavy Ion Transport Monte Carlo code. *JNST*, 39:1142–51, 2002.
- [12] D. B. Pelowitz. *MCNPX user's manual*. Los Alamos National Laboratory, 2005. [Online] Available: <http://mcnpx.lanl.gov>.

- [13] A. V. Dementyev and N. M. Sobolevsky. SHIELD — universal Monte Carlo hadron transport code: scope and applications. *Radiat. Meas.*, 30(5):553–557, 1999.
- [14] Irena Gudowska, Nikolai Sobolevsky, Pedro Andreo, Dževad Belkić, and Anders Brahme. Ion beam transport in tissue-like media using the monte carlo code SHIELD-HIT. *Phys. Med. Biol.*, 49:1933–1958, 2004.
- [15] M. H. Salamon. Range-Energy Program for relativistic heavy ions in the region  $1 < E < 3000$  MeV/amu. LBL Report LBL-10446, Lawrence Berkeley Lab, California Univ., Berkeley (USA), 1980.
- [16] T. Hiraoka and H. Bichsel. Stopping powers and ranges for heavy ions. *Jpn. J. Med. Phys.*, 15:91, 1995.
- [17] ICRU Report 49. *Stopping powers and ranges for protons and alpha particles*. International Commission on Radiation Units and Measurements, Bethesda, MD, 1993.
- [18] Niels Bassler, Oliver Jäkel, Christian Skou Søndergaard, and Jørgen B. Petersen. Dose- and LET-painting with particle therapy. *Acta Oncol.*, 49:1170–1176, 2010.
- [19] Hugo Palmans and Frank Verhaegen. Monte carlo study of fluence perturbation effects on cavity dose response in clinical proton beams. *Phys. Med. Biol.*, 43(1):65, 1998.
- [20] H. Palmans and S Vynckier. Reference dosimetry for clinical proton beams. In Jan P. Seuntjens and Paul N. Mobit, editors, *Recent Developments in Accurate Radiation Dosimetry*. Madison, WI: Medical Physics Publishing, 2002.
- [21] Joakim Medin and Pedro Andreo. Stopping powers for the ion-chamber dosimetry of radiotherapeutic heavy-particle beams. *Nucl. Instrum. Methods Phys. Res. B*, 69(1):64 – 75, 1992.
- [22] Nikolai Sobolevsky. SHIELD-HIT Home page, 2010. [Online] latest status: <http://www.inr.ru/shield/> [17 September 2018].
- [23] David C. Hansen, Armin Lühr, Rochus Herrmann, Nikolai Sobolevsky, and Niels Bassler. Recent improvements in the SHIELD-HIT code. *Submitted to International Journal of Radiation Biology*, 2011.
- [24] David C. Hansen, Armin Lühr, Nikolai Sobolevsky, and Niels Bassler. Benchmarking nuclear models in SHIELD-HIT. in preparation.
- [25] M. Krämer, O. Jäkel, T. Haberer, G. Kraft, D. Schardt, and U. Weber. Treatment planning for heavy-ion radiotherapy: physical beam model and dose optimization. *Phys. Med. Biol.*, 45:3299–3317, 2000.
- [26] M. Krämer and M. Scholz. Treatment planning for heavy-ion radiotherapy: calculation and optimization of biologically effective dose. *Phys. Med. Biol.*, 45:3319–3330, 2000.
- [27] Uli Weber and Gerhard Kraft. Design and construction of a ripple filter for a smoothed depth dose distribution in conformal particle therapy. *Phys. Med. Biol.*, 44:2765–2775, 1999.
- [28] Niels Bassler, Ioannis Kantemiris, Julia Engelke, Michael Holzscheiter, and Jørgen B. Petersen. Comparison of optimized single and multifield irradiation plans of antiproton, proton and carbon ion beams. *Radiother. Oncol.*, 95:87–93, 2010.
- [29] Johanna Kempe and Anders Brahme. Energy-range relation and mean energy variation in therapeutic particle beams. *Med. Phys.*, 35(1):159–170, 2008.
- [30] H. Bethe. Zur Theorie des Durchgangs schneller Korpuskularstrahlen durch Materie. *Ann. Phys.*, 5:325, 1930.
- [31] H. Bethe. Bremsformel für Elektronen relativistischer Geschwindigkeit. *Z. Phys.*, 76:293, 1932.
- [32] N. Bohr. The penetration of atomic particles through matter. *Kgl. Danske Videnskab. Selskab Mat.-Fys. Medd.*, 18(8), 1948. This reference has long been difficult to obtain, but can now be downloaded from: [http://www.sdu.dk/Bibliotek/E-hotel/MatFys.aspx?sc\\_lang=en](http://www.sdu.dk/Bibliotek/E-hotel/MatFys.aspx?sc_lang=en).
- [33] U. Fano. Penetration of protons, alpha particles, and mesons. *Annu. Rev. Nucl. Sci.*, 13:1, 1963.
- [34] J. Lindhard and M. Scharff. Energy dissipation by ions in the keV region. *Phys. Rev.*, 124(1):128–130, 1961.
- [35] ICRU Report 37. *Stopping powers for electrons and positrons*. International Commission on

- Radiation Units and Measurements, Bethesda, MD, 1984.
- [36] P. Sigmund, A. Schinner, and H. Paul. Errata and Addenda: ICRU Report 73 (Stopping of ions heavier than helium), 2009. [Online] Available: [http://www.icru.org/index.php?option=com\\_content&task=view&id=167](http://www.icru.org/index.php?option=com_content&task=view&id=167).
  - [37] Helmut Paul and Andreas Schinner. Empirical stopping power tables for ions from  ${}^3\text{Li}$  to  ${}^{18}\text{Ar}$  and from 0.001 to 1000 MeV/nucleon in solids and gases. *At. Data Nucl. Data Tables*, 85:377, 2003. Available from <http://www-nds.iaea.or.at/stoppinggraphs/>.
  - [38] Jakob Toftegaard, Armin Lühr, and Niels Bassler. *libdEdx*, 2010. [Online] Available: <http://sourceforge.net/projects/libdedx/> [17 September 2018].
  - [39] Armin Lühr, Jakob Toftegaard, Ioannis Kantemiris, and Niels Bassler. Stopping power: the generic library libdedx and a study of clinically relevant stopping-power ratios for different ions, 2011.
  - [40] M. J. Berger, J. S. Coursey, M. A. Zucker, and J. Chang. ESTAR, PSTAR, and ASTAR: Computer programs for calculating stopping-power and range tables for electrons, protons, and helium ions (version 1.2.3), 2005. [Online] Available: <http://physics.nist.gov/Star> [17 September 2018].
  - [41] T. Elsässer, A. Gemmel, M. Scholz, D. Schardt, and M. Krämer. The relevance of very low energy ions for heavy-ion therapy. *Phys. Med. Biol.*, 54(7):N101, 2009.
  - [42] F. Hubert, Rimbot R., and H. Gauvin. Semi-empirical formulae for heavy ion stopping powers in solids in the intermediate energy range. *Nucl. Instrum. Methods Phys. Res. B*, 36:357, 1989.
  - [43] Jens Lindhard and Allan H. Sørensen. Relativistic theory of stopping for heavy ions. *Phys. Rev. A*, 53:2443, 1996.
  - [44] Oksana Geithner. *Monte Carlo simulations for heavy ion dosimetry*. PhD thesis, University of Heidelberg, Germany, 2006.
  - [45] Dževad Belkić. Review of theories on ionization in fast ion-atom collisions with prospects for applications to hadron therapy. *J. Math. Chem.*, 47:1366, 2010.
  - [46] Phillip J. Taddei, Zhongxiang Zhao, and Thomas B. Borak. A comparison of the measured responses of a tissue-equivalent proportional counter to high energy heavy (HZE) particles and those simulated using the Geant4 Monte Carlo code. *Radiat. Meas.*, 43(9-10):1498 – 1505, 2008.
  - [47] ICRU Report 63. Nuclear data for neutron and proton radiotherapy and for radiation protection. Technical Report 63, International Commission on Radiation Units and Measurements, 2000.
  - [48] Peter Sigmund, 2010. Private communication.
  - [49] Harald Paganetti. Dose to water versus dose to medium in proton beam therapy. *Phys. Med. Biol.*, 54(14):4399, 2009.